Condensed Matter Physics 2008, Vol. 11, No 3(55), pp. 473–482

CONDENSED MATTER PHYSICS

X-ray photoelectron spectroscopy of $Sn_2P_2S_6$ crystals

J.Grigas[1], E.Talik[2], V.Lazauskas[3], Yu.M.Vysochanskii[4], R.Yevych[4], M.Adamiec[2], V.Nelkinas[3]

[1] Faculty of Physics, Vilnius University, Sauletekio 9/3, LT–10222 Vilnius, Lithuania

[2] Institute of Physics, Silesian University, Universytetska 4, 40–007 Katowice, Poland

[3] Institute of Theoretical Physics and Astronomy, Vilnius University, Gostauto 12, LT–01108 Vilnius, Lithuania

[4] Uzhgorod University, Pidhirna 46, 88000 Uzhgorod, Ukraine

Received April 24, 2008

The paper presents the X-ray photoelectron spectra (XPS) of the valence band (VB) and of the core levels (CL) of uniaxial ferroelectric $Sn_2P_2S_6$ single crystals from different crystallographic planes in both paraelectric and ferroelectric phases. The XPS were measured with monochromatized Al K_α radiation in the energy range 0–1400 eV. The VB consists of five bands with the maxima between 3.3 eV and 14.5 eV below the Fermi level. Experimental energies of the VB and core levels are compared with the results of theoretical *ab initio* calculations of the molecular model of the $Sn_2P_2S_6$ crystal. The electronic structure of the VB is revealed. Ferroelectric phase transition changes the atom's charge and strength of the bonds, electronic structure of VB, width of CL lines and chemical shifts for the Sn, P and S states which are crystallographic plane-dependent.

Key words: *$Sn_2P_2S_6$, ferroelectric crystals, XPS, electronic structure*

PACS: *71.20.-b, 77.84.-s, 78.70.En, 79.60.-i*

1. Introduction

Professor Ihor Stasyuk, whom we want to honour with this paper, was the first to show the possibility of soft mode frequency splitting by high unharmonicity near the Curie temperature in a ferroelectric semiconductor SbSI [1]. One of the split mode components drops to microwave range and causes high static permittivity. Later, X-ray photoelectron spectroscopy revealed a huge crystallographic plane-dependent splitting of the core-level binding energies in SbSI [2] crystals. $Sn_2P_2S_6$ is another well-known ferroelectric semiconductor where the soft phonon mode frequency decreases down to the millimetre range near T_c, causing an extremely high static permittivity. Ferroelectric properties in ferroelectric semiconductors are closely related to an electronic subsystem.

Ferroelectric and structural properties of $Sn_2P_2S_6$ are discussed in detail in the monograph [3]. The room-temperature ferroelectric (FE) phase is a monoclinic one, with the space group Pc. Above $T_c = 337$ K, the crystal undergoes the second order ferroelectric phase transition to paraelectric (PE) space group $P2_1/c$. At T_c, all four Sn atoms are shifted significantly in the [100] direction, with respect to the locations in the centrosymmetric state. The two non-equivalent Sn atoms are shifted by 0.325 Å along a, by 0.044 Å along b and by 0.094 Å along c and by 0.225 Å along a, by 0.044 Å along b and by 0.033 Å along c direction, respectively. Two pairs of Sn atoms have different shifts in the FE phase. This is related to nonlinear interaction of soft B_u mode and full symmetrical A_g mode in the PE phase. This interaction is very important for the phase transition nature. Changes in the position of P and S atoms at T_c are small. Thus, Sn atoms shift mainly along the [100] direction and this enables us to consider the Sn sublattice as ferroactive.

However, electronic properties of this crystal were less studied than structural and phonon properties. Electronic structure of $Sn_2P_2S_6$ was studied by X-ray photoelectron and X-ray fluorescence spectroscopes in combination with the full-potential linearized augmented plane-wave (FLAPW) band-structure calculations only in FE phase [4]. Due to a relative complexity and low symmetry of the crystal, one can expect different XPS from different crystal planes (as in SbSI [2]) as well as

in PE and FE phases. We failed to find any studies of the ferroelectric phase transition effect on the electronic structure of this crystal.

The purpose of this paper is to study XPS and electronic structure of the ferroelectric $Sn_2P_2S_6$ crystals in both FE and PE phases, and to reveal the effect of the ferroelectric phase transition on the electronic structure of the valence band and on the shifts in the core-level binding energies.

2. Experimental details

The $Sn_2P_2S_6$ crystal was grown by vapour transport. The XPS of valence band and principal core levels were measured using a PHI 5700/660 Physical Electronics Spectrometer with monochromatic Al K_α radiation (1486.6 eV) of 0.3 eV full width at half maximum. The photoelectron spectra as a function of kinetic energy were analysed in the energy range 0–1400 eV by a hemispherical mirror analyser. All spectra are obtained using 400-μm-diameter analysis area. The measurements were performed from the crystallographic planes, perpendicular to ferroelectric x- and z-axes, and non-ferroelectric y-axis, cleaved *in situ* in the low 10^{-10} torr range vacuum to obtain the clean surfaces. The survey spectra taken directly after breaking the crystal showed small contamination of oxygen and a rather low one of the carbon that should have no effect on the VB and CL spectra. The angle was 45° between the sample and X-ray incident beam. A charging effect was observed. However, all spectra were corrected for this charging effect using the carbon 1s line of adsorbed carbon ($E_b = 285$ eV).

3. Molecular model of $Sn_2P_2S_6$ crystal and *ab initio* calculations of the energy levels

The electronic structure of the VB and CL was calculated using the method based on solutions of restricted Hartree-Fock (RHF) equations, in the Linear Combinations of Atomic Orbitals (LCAO) approach for the molecular orbitals (MO). According to the Koopmans' theorem, the one-particle energies obtained from the canonical RHF equations correspond to the approximate energies of the ionization potential. This would be an exact solution if the ionization process was instantaneous and the correlation energy contribution could be completely neglected.

To calculate the energy levels we need a molecular model of the crystal. The model should be a cluster composed of an even number of molecules. However, the interactions between the clusters are not as weak as they should be. Figure 1 shows a fragment of the crystal structure on the xy plane in FE phase. The unit cell is shadowed. This selected $Sn_4(P_2S_6)_4$ cluster gives a stable RHF solution. Such a cluster was used for theoretical calculations.

Table 1. Strength of Sn-S bonds in FE and PE phases. Numbers of atoms are given in figure 1.

Sn1–S	FE	PE	Sn2–S	FE	PE	Sn3–S	FE	PE	Sn4–S	FE	PE
1–9	0.41	0.56	2–10	0.55	0.40	3–11	0.19	0.24	4–13	0.23	0.36
1–15	0.10	0.24	2–11	0.48	0.36	3–17	0.19	0.56	4–15	0.35	0.36
1–30	0.42	0.42	2–19	0.45	0.36	3–26	0.05	0.29	4–18	0.32	0.40
1–33	0.38	0.24	2–31	0.36	0.32	3–27	0.07	0.24	4–27	0.46	0.24
1–35	0.43	0.29	2–33	0.10	0.24	3–32	0.28	0.42	4–29	0.33	0.32

The molecular orbital (MO) is a linear combination of atomic orbitals (AO). The MO (φ_i) can be expanded by the AO ($\chi_\mu(\mathbf{r})$) base:

$$\varphi_i(\mathbf{r}) = \sum_{\mu=1}^{M} C_{i\mu}\chi_\mu(\mathbf{r}), \tag{1}$$

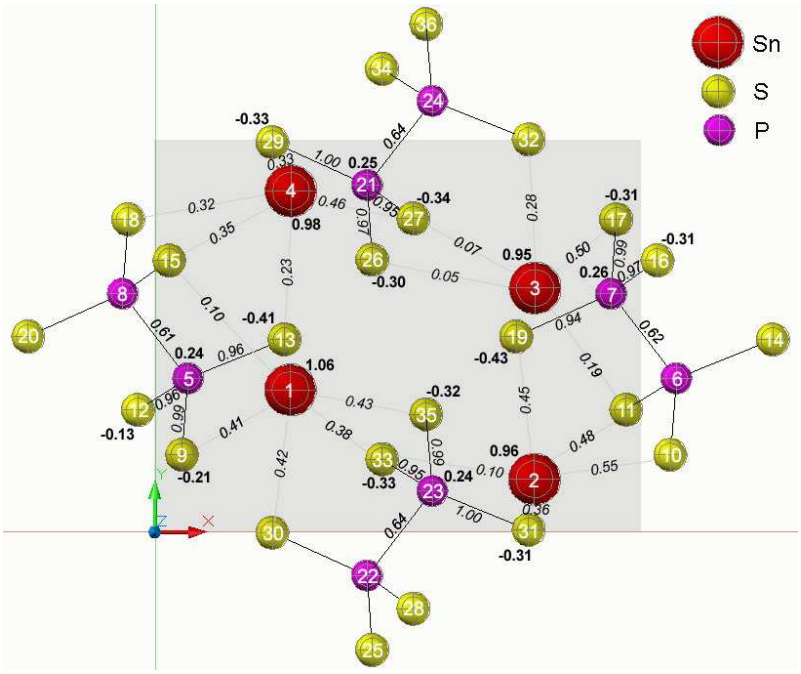

Figure 1. $Sn_8(P_2S_6)_8$ cluster as a molecular model of $Sn_2P_2S_6$ crystal on the xy plane. The calculated bond strengths and atom's charges in the FE phase are shown in the picture.

where μ is the number of the AO, or the set of quantum numbers (nlm). The $\mathbf{C}$ matrix is obtained by solving Hartree-Fock matrix equation

$$\mathbf{FC} = \mathbf{SC}\varepsilon. \tag{2}$$

The method of solving equation (2) as well as calculations of the binding energy, bond strength and atomic charge are described in [2]. The calculations were performed using the GAMESS program [5]. The calculated bond strengths and the Mulliken charge of the atoms in the FE phase are shown in figure 1. In this model, Sn atom's charge is close to +1 and the crystal is ionic $Sn_2^{2+}(P_2S_6)^{2-}$. At the FE phase transition, the strength of the bonds as well as the charge of atoms change. Most of the changes occur in Sn3 surroundings. These changes are given in table 1. These results show that the rearrangement of most of the bonds takes place at the ferroelectric phase transition. The valency of ferroactive Sn ions also changes: Sn1 is 3.03 and 2.99, Sn2 is 2.81 and 2.72, Sn3 is 1.92 and 2.99, and Sn4 is 2.81 and 2.72 in the PE and FE phase, respectively. The valency and charge of Sn3 ions change at phase transition most of all, i.e. they decrease in the FE phase (charge decreases from 1.07 to 0.95).

Table 2. Values of the calculated binding (negative) energies (eV).

State	FE phase	PE phase
Sn 3s	860.7–859.7	860.3–860.2
Sn 3p	741.2–740.1	740.8–740.7
Sn 3d	520.2–519.1	519.8–519.7
S 2s	246.3–240.1	244.9–241.4
P 2s	210.1–207.9	209.5–208.8
S 2p	182.3–175.9	180.8–177.2
Sn 4s	153.1–152.1	152.7–152.7
P 2p	151.9–149.7	151.4–150.6
Sn 4p	111.2–110.1	110.8–110.7
Sn 4d	40.5–39.4	40.1–39.9

Table 2 presents theoretical values of the binding energies of the $Sn_4(P_2S_6)_4$ cluster without taking into account the spin-orbit interaction. The quantum-mechanical method and the chosen cluster give higher negative CL as well as VB energies than their experimental values (see table 3). Nevertheless, the cluster reflects the electronic structure and binding energies of the crystal.

Table 3. Binding energies and chemical shifts of atoms at different planes in FE (RT) and PE (360 K) phases (eV).

Peak	y,z-plane RT	y,z-plane 360 K	x,y-plane RT	x,y-plane 360 K	x,z-plane RT	x,z-plane 360 K
P $2p_{3/2}$ in compound	132.0	131.8	132.6	132.1	132.3	131.8
P $2p_{3/2}$ in literature				130.0		
chemical shift	2.0	1.8	2.6	2.1	2.3	1.8
P $2p_{1/2}$ in compound	132.9	132.6	133.5	133.0	133.2	132.6
P $2p_{1/2}$ in literature				131.0		
chemical shift	1.9	1.6	2.5	2.0	2.2	1.6
S $2p_{3/2}$ in compound	162.3	161.9	162.7	162.3	162.4	161.7
S $2p_{3/2}$ in literature				164.0		
chemical shift	−1.7	−2.1	−1.3	−1.7	−1.6	−2.3
S $2p_{1/2}$ in compound	163.5	163.0	163.9	163.5	163.6	162.9
S $2p_{1/2}$ in literature				165.0		
chemical shift	−1.5	−2.0	−1.1	−1.5	−1.4	−2.1
Sn $3d_{5/2}$ in compound	486.7	486.5	486.9	486.3	486.8	486.3
Sn $3d_{5/2}$ in literature				485.0		
chemical shift	1.7	1.5	1.9	1.3	1.8	1.3
Sn $3d_{3/2}$ in compound	495.1	494.9	495.3	494.7	495.5	494.6
Sn $3d_{3/2}$ in literature				493.0		
chemical shift	2.1	1.9	2.3	1.7	2.5	1.6

4. Results of XPS and electronic structure

4.1. Survey spectra

Figure 2 shows the XPS of the $Sn_2P_2S_6$ crystal in the energy range from 0 to 1400 eV below the Fermi level both in the PE (360 K) and FE (RT) phases from the crystallographic xz plane. Only small amounts of oxygen (O $1s$) and carbon (C $1s$) have been detected. The spectra from other crystallographic planes are similar. Inelastically scattered electrons give the background. Auger spectra of Sn MNN, of S LMM and C KLL are also seen in the high energy range. The strongest peaks of Sn $3d$, Sn $4d$, Sn $3p$, P $2p$, S $2p$ were chosen for investigation of peculiarities of the crystallographic plane-dependent core-level XPS in this ferroelectric semiconductor.

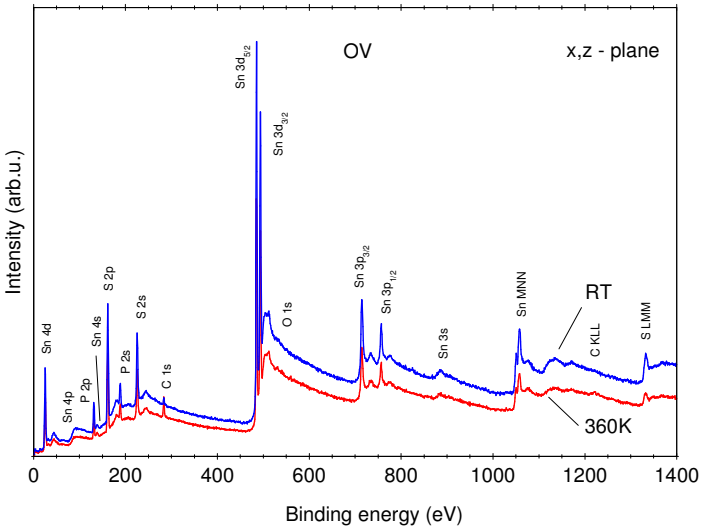

Figure 2. Overview spectra of $Sn_2P_2S_6$ crystal from the xz plane in the PE (360 K) and FE (RT) phases.

4.2. Valence band

X-ray photoelectron spectroscopy of the valence band provides data of the occupied total density of states. Figure 3 shows the VB spectra both in the PE and FE phases. The VB consists of five distinguishable bands with the maximum intensity at 2.8 eV, 6.7 eV, 9.2 eV, 11.0 eV, and 14.0 eV. In FE phase the energies are shifted by approximately 0.5 eV to higher values and coincide with those obtained in [4]. In the PE phase, the VB is separated by a gap of about 1.1 eV from the Fermi level. In the ferroelectric RT phase, the VB is located at about 1.5 to 22 eV below E_F. In

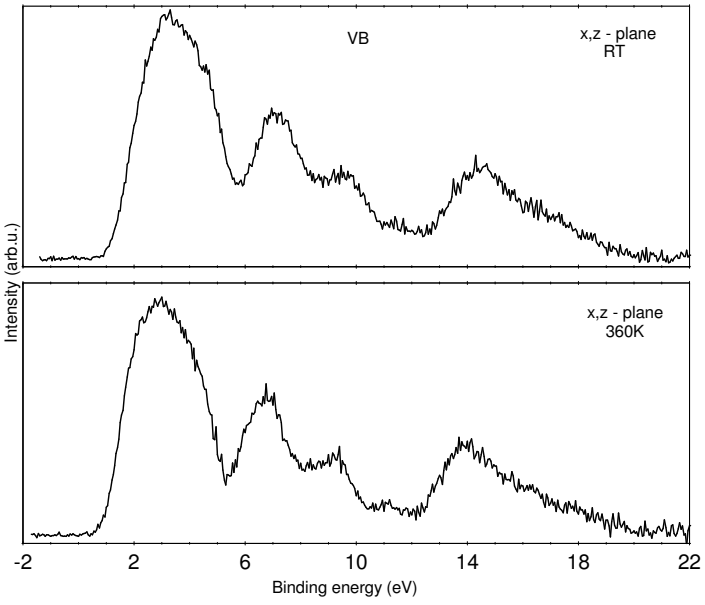

Figure 3. XPS of VB from the xz plane in the PE (360 K) and FE (RT) phases.

these crystals, the optical band gap at room temperature is 2.3 eV. It means that the Fermi level is pinned nearly in the middle of the band gap.

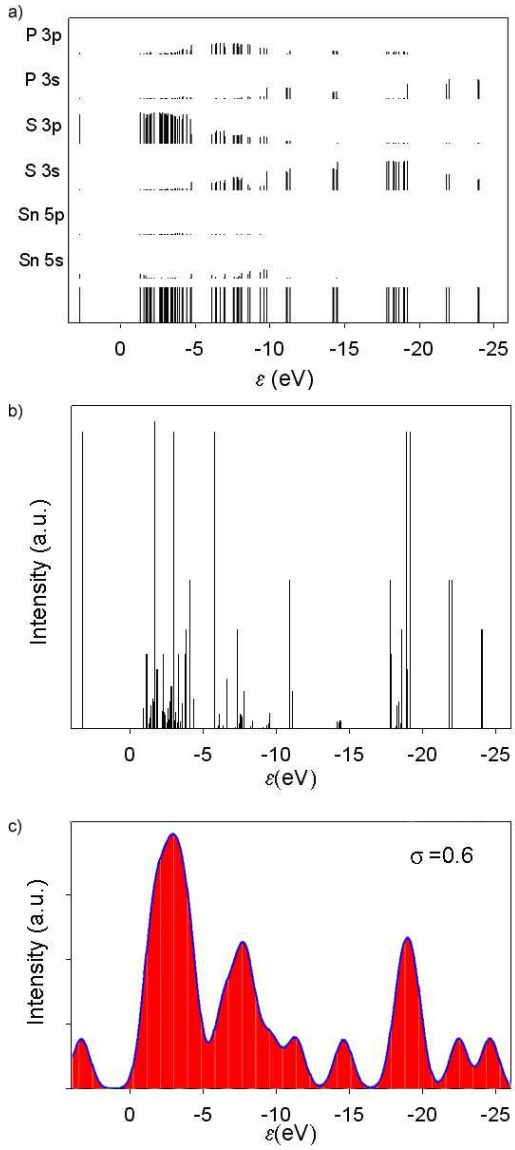

Figure 4. Electronic structure of VB in PE phase: (a) DOS band and contribution of states (%); (b) intensity of DOS. In equation (3) $\Delta\varepsilon = 0.0027$ eV; (c) calculated VB for $Sn_4(P_2S_6)_4$ cluster and approximated by equation (4).

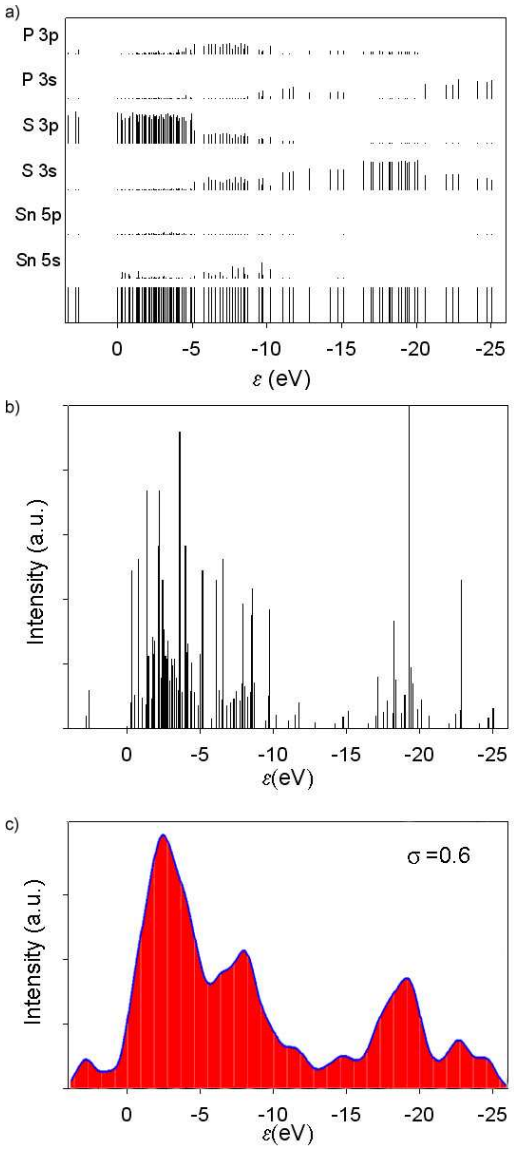

Figure 5. Electronic structure of VB in FE phase. Designations are the same as in figure 4. In equation (3) $\Delta\varepsilon = 0.021$ eV, therefore the intensities are lower and minima are shallower than in PE phase.

Figure 4 shows the calculated PE phase VB form and electronic structure of $Sn_2P_2S_6$ crystal. The reference point of the prectrum is at the Fermi level (E_F). The E_F was determined experimentally with the accuracy of 0.3 eV. The intensities of the XPS were described in three ways:

(a) By the energy states band ε_i from the characteristic equation (2).

(b) By the peaks of the density of states:

$$D(\varepsilon) = \frac{1}{N_M}\frac{1}{\Delta\varepsilon}, \tag{3}$$

where N_M is the number of molecules in the cluster.

(c) By the Gaussian broadening method:

$$D(\varepsilon) = \frac{1}{\sqrt{2\pi\sigma}} \sum_i \exp\left(-\frac{(\varepsilon - \varepsilon_i)^2}{2\sigma^2}\right), \tag{4}$$

where the sum is performed over the states i, and ε_i are the corresponding energy levels, and σ is the half-width of the Gaussian function.

The form of the VB can be explained by the analysis of MO population. Knowing the MO normalized coefficients $C_{i\mu}$ (equation (1)), we can evaluate the contribution of the A atom electrons to ε_i state:

$$p_{iA} = \sum_{\mu \in A} C_{i\mu}^2. \tag{5}$$

From the partial density of states (PDOS) (in %) calculated by equation (5) and the total density of states (a), the representation D(ε) for the peaks (b) of the DOS (equation (3)) and approximation of the bands spectra (c) by the Gaussian broadening method (equation (4)) for $Sn_4(P_2S_6)_4$ molecular cluster it follows that from 4 to 2 eV is the conduction band (CB), the right edge of which forms S 3p electrons. Unlike SbSI [3] crystals, the VB consists of five bands. It is dominated by Sn 5s, Sn 5p, S 3s, S 3p, P 3s and P 3p states. Five DOS peaks are degenerated. The main contribution to the most intensive band between -1 and -5 eV gives S 3p states. The left edge of this band forms S 3p states with 13% Sn 5s and few percent P 3p states. The main contribution to the next intensive band between -5 and -12 eV comes from S 3s, S 3p, P 3p and Sn 5s states. Sn 5s and 5p states give only a small contribution to the first two bands. The low-energy part of VB is formed mainly by S 3s and P 3s states; S 3s electrons form a band at -14 eV, while P 3s electrons form a band at -18.5 eV. Above -25 eV there dominate P 3s with mixture of S 3s states. The five experimental bands at -3.3 eV, -7.2 eV, -9.7 eV, -11.5 eV and -14.5 eV are in good agreement with [4].

The calculated bands are shifted to higher energies, however. It means that electron-electron interactions are overestimated. CL electrons extend the VB to higher energies. This is also confirmed experimentally. Higher-energy edges of all the bands are sloppier. The last three high-energy bands are experimentally seen as one diffused band. Tin atoms are strongly ionized. The electron density from Sn goes primarily to the neighboring S atoms, yielding nearly full occupation of the S 3p band. The calculated PDOS in this approach slightly differs from the FLAPW calculations [4]. However, the main VB features are the same. Intensity of DOS is higher and minima are deeper than in FE phase. The FE phase DOS band is rarefied in comparison with PE phase DOS.

Figure 5 shows the calculated VB form and electronic structure of FE phase. The gap between the VB and CB decreases from 4.1 eV (in PE phase) to 2.6 eV. The calculated width of the VB is 24.9 eV, while in PE phase it is 23.1 eV. In FE phase, there is only one quasi-degenerated state instead of five in PE phase. Disappearance of centro-symmetry abolishes the degenerated electronic states. The left edge of the most intensive band between -1 and -5 eV forms S 3p states with few percent of P 3p states. Sn 5s states disappear. The phase transition changes the electronic structure of the crystal by changing PDOS of all the atoms.

Mechanism of the formation of an electron lone pair of tin cations, which is related to the appearance of spontaneous polarization [6], could be used in explaining the evolution of VB spectra at transition from PE phase to FE phase (figure 3). The hybridization of sp^2 type determines the peculiarities of the density of states in VB. Antibonding mixing of Sn 5s–S 3p orbitals produces states at the top of VB. Bonding interaction of Sn 5p orbitals with previous antibonding Sn 5s–S 3p states generates lower energy filled states Sn 5p + (Sn 5s–S 3p), or shortly sp^2. This way, the gain of electronic subsystem energy is determined. Lowering of the energy of these sp^2 states is proportional to acentricity of the surrounding of Sn ions (similarly to the known Jahn-Teller effect). Such a formation of the Sn lone pair electron "cloud" together with deformation of the nearest polyhedron of sulfur atoms determine the origin of spontaneous polarization. So, at transition to FE phase and at the increase of spontaneous polarization, the hybridization sp^2 becomes stronger and this causes the lowering of the density of electronic states at the top of the VB. This way could

be interpreted the observed lowering of energy of the band with maximum near 3 eV in the VB XPS spectra (figure 3) on cooling from 360 K to RT.

4.3. Core levels

Figures 6 and 7 show the spectra of the Sn 3*d* and Sn 4*d* spin-orbit doublets from the xz plane in the FE and PE phases. In the FE phase, all the CL bands are broader than in PE phase. The stronger interactions are observed for the polar yz plane.

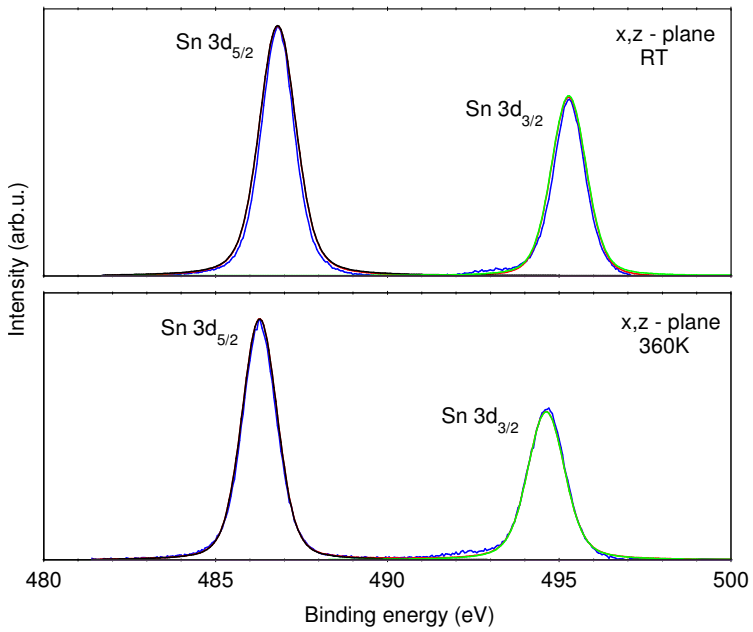

Figure 6. XPS of Sn 3*d* spin-orbit doublet in FE (RT) and PE (360 K) phases.

Sn 3*d* spectra in the PE phase are fitted by one doublet, but in the FE phase they could be better fitted by two doublets. The effect of the phase transition for the Sn 3*d* levels is small in comparison with the observed change for the Sn 4*d* XPS spectra.

In the PE phase, all Sn ions are equivalent while in the FE phase, two nonequivalent pairs of Sn ions already exist. So, Sn 4*d* RT spectra could be fitted by two doublets with the splitting 1.03 eV

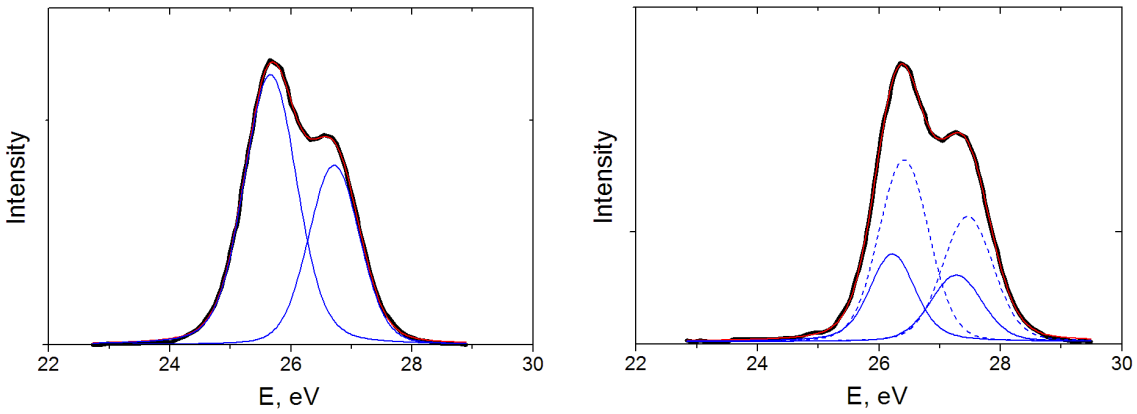

Figure 7. XPS of Sn 4*d* spin-orbit doublet in (left) PE and (right) FE phases.

like in PE phase. In FE phase, anisotropy of XPS spectra is clearly seen. The observed difference for the XPS Sn 4*d* spectra registered from X, Y and Z cuts in FE phase could be related to the shape of the domain walls and to their different concentration on crystal surfaces. Also, for the planes (010) perpendicular to Y direction, with variation of their position, different nonequivalent pairs of Sn atoms are placed near the surface. For Z cut, both types of Sn nonequivalent atoms simultaneously locate at the surface. Probably this structure peculiarity determines a bigger difference in the spectral area for the doublets in Sn 4*d* Y-cut RT spectra.

Anisotropy could be explained as a result of different types of Sn ions placed at the surface. In FE phase, the macroscopic field of spontaneous polarization also modifies the surface properties [2] differently for the polar and non-polar planes. Therefore, XPS from different planes slightly differ (figure 8). On the Sn/Ge (111) surface [7] three components in the line shape of the Sn 4*d* core level also reflect the three inequivalent positions of the Sn atoms that form the unit cell.

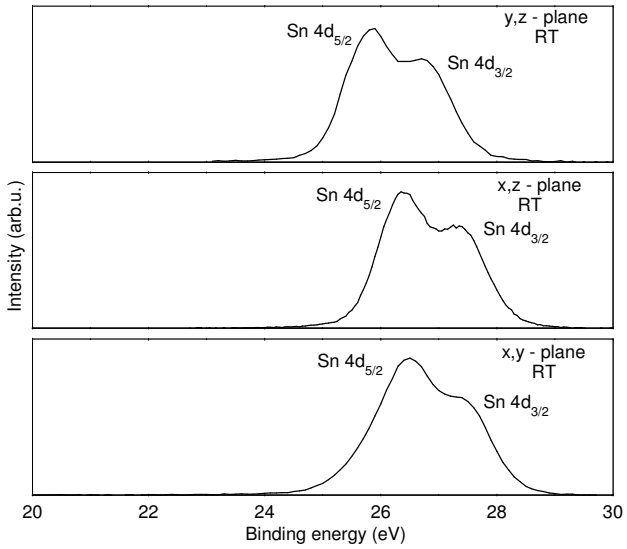

Figure 8. XPS of Sn 4*d* spin-orbit doublet from different planes in FE (RT) phase.

The experimental binding energies and chemical shifts of atoms at different planes both in the FE (RT) and PE (360 K) phases are given in table 3. The electronic structure measurements revealed the chemical shifts of Sn and P states to a higher binding energy and of S states to a lower binding energy. This shift suggests a charge transfer from Sn and P to S atoms. However, the binding energies and chemical shifts are crystallographic plane-dependent. Also, they change at the ferroelectric phase transition. In the FE phase, the chemical shifts of Sn and P atoms are higher while those of S atoms are smaller. Due to the inequivalent positions of the Sn atoms in FE phase, the line width in FE (RT) phase significantly increases mainly in xy plane.

5. Conclusions

X-ray photoelectron spectra of the valence band and of the core levels of the semiconductor ferroelectric $Sn_2P_2S_6$ crystal are presented in the energy range from 0 to 1400 eV. A molecular model of the crystal is used for *ab initio* theoretical calculations of the binding energies. Theoretical values of the binding energies are close to the experimental ones. The structure of valence band is calculated and confirmed experimentally. The XPS studies revealed the crystallographic plane-dependent binding energies and chemical shifts which also change at the ferroelectric phase transition. The ferroelectric phase transition changes the electronic structure of VB. The appearance of inequivalent positions of Sn atoms in FE phase splits the spin-orbit doublets of Sn 3*d* and 4*d* spectra.

Acknowledgements

This work was performed with financial support of the Lithuanian State Science and Studies Foundation and within the framework of the Lithuanian-Ukrainian project.

References

1. Grigas J., Kalesinskas V., Stasyuk I., Ferroelectrics, 1984, **55**, 31.
2. Grigas J., Talik E., Lazauskas V., Lithuanian Journal of Physics, 2004, **44**, 427.
3. Vysochanskii Yu.M., Janssen T., Currat R., Folk R., Banys J., Grigas J., Samulionis V. Phase Transitions in Ferroelectric Phosphorous Chalcogenide Crystals. Vilnius University Publ. House, Vilnius, 2006, p. 453
4. Kuepper K., Shneider B., Caciuc V., Neumann M., Postnikov A.V., Ruediger A., Grabar A.A., Vysochanskii Yu.M., Phys. Rev. B, 2003, **67**, 115101.
5. Schmidt M.W., Baldrige K.K., Boatz J.A., Elbert S.T., Gordon M.S., Jensen J.H., Koseki S., Matsunaga N., Nguyen K.A., Su S., Windus T.L., Dupuis M., Montgomery J.A., J. Comput. Chem., 1993, **14**, 1347.
6. Rushchanskii K.Z., Vysochanskii Yu.M., Strauch D., Phys. Rev. Lett., 2007, **99**, 207601.
7. Tejeda A., Cortés R., Lobo-Checa J., Didiot C., Kierren B., Malterre D., Michel E.G., Mascaraque A., Phys. Rev. Lett., 2008, **100**, 026103.

Рентгенівська фотоелектронна спектроскопія кристалів $Sn_2P_2S_6$

Й.Грігас[1], Е.Талік[2], В.Лазаускас[3], Ю.М.Височанський[4], Р.Євич[4], М.Адамєц[2], В.Нелкінас[3]

[1] Фізичний факультет, Вільнюський університет, вул. Саулетекіо 9/3, 10222 Вільнюс, Литва

[2] Інститут фізики, Сілезійський університет, вул. Університетьска 4, 40–007 Катовіце, Польща

[3] Інститут теоретичної фізики та астрономії, Вільнюський університет, вул. Гостауто 12, 01108 Вільнюс, Литва

[4] Ужгородський університет, вул. Підгірна 46, 88000 Ужгород, Україна

Отримано 24 квітня 2008 р.

У статті представлено рентгенівські фотоелектронні спектри (РФЕС) валентної зони (ВЗ) та остовних рівнів (ОР) одновісних сегнетоелектричних кристалів $Sn_2P_2S_6$, отримані з різних кристалографічних площин і в параелектричній, і в сегнетоелектричній фазах. РФЕС виміряно з використанням монохроматизованого Al K_α випромінювання в енергетичному діапазоні 0–1400 еВ. ВЗ містить п'ять підзон з максимумом між 3.3 еВ і 14.5 еВ нижче рівня Фермі. Експериментальні значення енергій рівнів ВЗ та ОР порівняно з результатами теоретичних розрахунків з перших принципів для молекулярної моделі кристалу $Sn_2P_2S_6$. Визначено електронну структуру ВЗ. Перехід у сегнетоелектричну фазу змінює атомні заряди та міцність зв'язків, електронну структуру ВЗ, ширину ліній ОР та хімічні зсуви для станів Sn, P і S, що є залежними від кристалографічних площин.

Ключові слова: *$Sn_2P_2S_6$, сегнетоелектричні кристали, РФЕС, електронна структура*

PACS: *71.20.-b, 77.84.-s, 78.70.En, 79.60.-i*